Crystal structure of austinite, CaZn(AsO$_4$)OH

Lori A. Clark

Department of Geophysical Sciences, University of Chicago, Chicago, Illinois 60637, USA

Joseph J. Pluth, Ian Steele, Joseph V. Smith and Stephen R. Sutton

Department of Geophysical Sciences and Center for Advanced Radiation Sources, University of Chicago, Chicago, Illinois 60637, USA

Abstract

Austinite belongs to the adelite mineral group of calcium and lead arsenates, and has the conichalcite/descloizite type of crystal structure. The crystal structure of nearly pure austinite, CaZn(AsO$_4$)OH, was redetermined (R = 0.014) and the absolute configuration identified. The space group $P2_12_12_1$ and cell parameters a 7.5092(8), b 9.0438(9), c 5.9343(8) Å match previous data. Zinc octahedra share edges to form chains parallel to c. Arsenic tetrahedra share vertices with the Zn octahedra to generate a compact framework. Calcium square antiprisms share edges to make chains parallel to a that occupy the channels in the zinc-arsenic framework.

KEYWORDS: austinite, crystal structure, adelite group.

Introduction

ARSENIC is an environmental contaminant with sources that include the semiconductor industry (GaAs production), herbicides, pesticides and wood preservatives (Cu-Cr-As). Arsenic occurs naturally in lake waters and sediments from rock and soil weathering. Its high solubility and mobility, particularly of As(V), result in dangerous concentrations in some drinking waters. Knowledge of the crystal-chemistry of As-containing minerals is important for waste management.

The adelite mineral group contains seven arsenates ABAsO$_4$(OH): (A = Ca, B = Co, Cu, Zn, Mg, Ni; and A = Pb, B = Cu, Zn, Fe). They occur as secondary minerals in the oxide zone of base metal ore bodies (Magalhães et al., 1988; Crowley, 1975). From crystallographic data, they belong to the conichalcite/descloizite structure group with space group $P2_12_12_1$ (Richmond, 1940; Radcliffe and Simmons, 1971). Limited solid substitution occurs between most of the end members (Giuseppetti and Tadini, 1988; Fleischer, 1987; Jambor et al., 1980; Radcliffe and Simmons, 1971; Richmond, 1940).

The structure type of conichalcite was established by Qurashi and Barnes (1963a), and the structure of nickel-austinite was determined by Cesbron et al. (1987). The structure of austinite (mineralogical description; Staples, 1935) was determined accurately

by Giuseppetti and Tadini (1988), but the chemical composition of the single crystal was not measured. We determined the chemical composition of the single crystal used for diffraction, and established the absolute configuration of the asymmetric structure.

Experimental

Structure determination

The austinite came from Sonora, Mexico, [box of unclassified micromounts, Department of Geophysical Sciences, University of Chicago]. The apple-green crystals occur as sub-millimetre inter-grown tablets and prisms. The tip of a single, clear, rhombic prism (30 × 40 × 50 micrometre) was mounted on a glass fibre with epoxy. Initial data collected on the Laue experimental setup at beamline X26C of the National Synchrotron Light Source at Brookhaven National Labs, revealed sharp diffractions. Fluorescence analysed by a Si(Li) detector mounted 90° to the beam direction indicated considerable Zn and very little Cu.

At the University of Chicago, the crystal was mounted on an automated Picker-Krisel four-circle diffractometer with its prism axis (100) offset a few degrees from the ϕ axis. Refinement using 20 diffractions (24° < 2θ < 44°; k = 0.71073 Å), each the average of eight equivalent settings, gave

Table 1. Atomic coordinates

Atom	x/a	y/b	z/c	U_{eq}
As	0.62285(2)	0.67699(2)	0.51670(3)	5.93(5)
Zn	0.23594(3)	0.49358(3)	0.24316(4)	9.64(6)
Ca	0.63121(5)	0.32805(3)	0.47712(6)	9.77(9)
O(1)	0.4475(2)	0.5587(2)	0.4900(2)	10.5(2)
O(2)	0.7914(2)	0.5633(2)	0.5882(2)	14.0(3)
O(3)	0.3500(2)	0.2678(2)	0.2309(2)	10.7(3)
O(4)	0.3970(2)	0.2903(2)	0.7585(2)	11.9(3)
O(5)	0.1085(2)	0.4269(2)	0.5087(2)	8.8(3)
H	0.014(5)	0.473(3)	0.513(5)	27(8)

orthogonal cell parameters a 7.5092(8), b 9.0438(9), c 5.9343(8) Å. These values are similar to those for conichalcite (Qurashi and Barnes, 1963a), cobalt-austinite (Nickel and Birch, 1988), nickel-austinite (Cesbron *et al.*, 1987) and austinite (Giuseppetti and Tadini, 1988): 7.40, 7.50, 7.455(3), 7.505(1); 9.21, 9.01, 8.955(3), 9.037(2); 5.84, 5.92, 5.916(2), 5.921(1). The cell parameters and a subsequent electron-microprobe chemical analysis indicate that this crystal is austinite.

Collection of 5832 diffractions used the θ—2θ step-scan technique, 0.04°/step, counting for 1 sec/step, and scan width 4° with a 2θ range of 4—65°. Merging yielded 1465 diffractions (R_{int} = 0.032), all of which were used in the refinement. Three standard diffractions stayed constant, and the data collection range was $h \pm 11$, $k \pm 13$, $l \pm 8$. The absorption correction used a local program based on the analytical method for an ideal rhombic prism, with 0.50 and 0.28 as the maximum and minimum absorption corrections (μ = 15.44 mm^{-1}).

The systematic absences fitted $P2_12_12_1$, and Giuseppetti and Tadini's (1988) atomic coordinates were used for the initial model. Least-squares refinement against F^2 was performed using neutral scattering factors, and both isotropic and anisotropic

thermal parameters (SHELXL93; Sheldrick, 1993). A difference Fourier map revealed the hydrogen atom.

The final model with 81 refined parameters yielded weighted R (wR_2) of 0.036. The F (R$_1$) of 0.014 was much smaller than Giuseppetti and Tadini's (1988) calculated R$_1$ index of 0.033. Chiral inversion of the structure on the other hand resulted in an increase of wR_2 to 0.126, R$_1$ 0.038, S 3.8. The maximum and minimum heights on the final difference Fourier map +0.44 and −0.76 eÅ^{-3}. Local data reduction and cell refinement programs were used. Final atomic coordinates are give in Table 1, displacement parameters in Table 2 and bond distances and angles in Table 3.

Chemical analysis

The crystal used for data collection was mounted on a glass disk in a drop of 5-minute epoxy. The hardened epoxy was ground with 600 SiC grit paper until the crystal was slightly exposed. The crystal was then polished successively with 9, 6, and 1 μm diamond abrasive. Although several scratches and irregularities remained, concern for losing the crystal prevented further attempts to achieve a better

Table 2. Displacement parameters (× 10^3)

Atom	U_{11}	U_{22}	U_{33}	U_{23}	U_{13}	U_{12}
As	6.16(8)	6.12(8)	5.52(8)	0.14(5)	−0.04(6)	−0.80(5)
Zn	11.0(1)	11.6(1)	6.3(1)	1.67(6)	0.99(7)	−1.14(6)
Ca	10.4(2)	7.6(2)	11.4(2)	0.5(1)	1.1(1)	0.7(1)
O(1)	11.0(5)	10.8(5)	9.8(6)	0.4(5)	0.3(5)	−3.7(4)
O(2)	10.3(5)	14.7(6)	17.1(6)	0.7(5)	−2.5(5)	2.6(5)
O(3)	12.1(5)	11.6(5)	8.3(5)	−1.3(4)	1.0(4)	2.6(4)
O(4)	13.9(5)	12.5(5)	9.3(5)	2.8(4)	1.9(5)	2.6(4)
O(5)	8.9(5)	9.6(5)	7.8(5)	1.1(4)	−0.1(5)	0.1(4)

TABLE 3. Interatomic distances (Å) and bond angles (°)

Distances		Angles			
Ca−O(5)	2.313(1)	O(5)−Ca−O(4)	77.48(4)	O(1)−Ca−O(2)	63.48(4)
Ca−O(4)	2.449(1)	O(5)−Ca−O(1)	142.10(4)	O(1)−Ca−O(3)	128.33(4)
Ca−O(1)	2.502(1)	O(5)−Ca−O(2)	149.67(5)	O(1)−Ca−O(2)	80.42(4)
Ca−O(2)	2.531(1)	O(5)−Ca−O(3)	71.50(4)	O(1)−Ca−O(3)	75.32(4)
Ca−O(3)	2.540(1)	O(5)−Ca−O(2)	115.45(5)	O(1)−Ca−O(4)	139.88(4)
Ca−O(2)	2.575(1)	O(5)−Ca−O(3)	75.76(4)	O(2)−Ca−O(3)	78.57(4)
Ca−O(3)	2.625(1)	O(5)−Ca−O(4)	70.96(4)	O(2)−Ca −O(2)	78.78(3)
Ca−O(4)	2.661(1)	O(4)−Ca−O(1)	72.51(4)	O(2)−Ca −O(3)	134.56(4)
		O(4)−Ca−O(2)	106.33(5)	O(2)−Ca −O(4)	96.80(4)
		O(4)−Ca −O(3)	87.24(4)	O(3)−Ca−O(2)	126.57(5)
		O(4)−Ca −O(2)	145.72(5)	O(3)−Ca−O(3)	146.00(2)
		O(4)−Ca −O(3)	76.86(4)	O(3)−Ca−O(4)	74.70(4)
		O(4)−Ca −O(4)	147.20(2)	O(2)−Ca−O(3)	76.22(4)
				O(2)−Ca−O(4)	60.89(4)
				O(3)−Ca−O(4)	103.14(4)
Zn−O(5)	1.940(1)	O(5)−Zn−O(5)	171.08(5)	O(1)−Zn−O(4)	86.09(5)
Zn−O(5)	1.954(1)	O(5)−Zn−O(1)	100.84(5)	O(1)−Zn−O(3)	91.29(5)
Zn−O(1)	2.092(1)	O(5)−Zn−O(4)	91.09(5)	O(1)−Zn−O(1)	174.85(5)
Zn−O(4)	2.197(1)	O(5)−Zn−O(3)	86.02(5)	O(4)−Zn−O(3)	175.68(5)
Zn−O(3)	2.215(1)	O(5)−Zn−O(1)	84.30(5)	O(4)−Zn−O(1)	93.5(5)
Zn−O(1)	2.240(1)	O(5)−Zn−O(1)	88.03(6)	O(3)−Zn−O(1)	89.42(5)
		O(5)−Zn−O(4)	88.48(5)		
		O(5)−Zn−O(3)	94.87(5)		
		O(5)−Zn−O(1)	86.84(5)		
As−O(2)	1.685(1)	O(2)−As−O(4)	103.74(7)	O(4)−As−O(3)	113.66(6)
As−O(4)	1.689(1)	O(2)−As−O(3)	115.04(7)	O(4)−As−O(1)	112.72(6)
As−O(3)	1.696(1)	O(2)−As−O(1)	102.77(7)	O(3)−As−O(1)	108.44(6)
As−O(1)	1.704(1)				
H−O(5)	0.82(3)	O(5)−H−O(2)	167(3)		
H−O(2)	1.91(3)				
O(5)−O(2)	2.723(2)				

surface. The polished mount was carbon coated and analysed with a Cameca SX-50 electron microprobe. Visual analysis of the energy-dispersive spectrum indicated only Cu, Ca, Zn, As, and Mg. Standards for wavelength-dispersive analysis included copper metal, anorthite ($CaAl_2Si_2O_8$), ZnO, $FeAs_2$ and diopside ($CaMgSi_2O_6$).

Variation in three analyses at points selected to minimize imperfections results from poor polishing rather than variable chemistry. The average (Table 3) corresponds to $Ca(Zn_{0.95}Cu_{0.03}Mg_{0.02})AsO_4(OH)$. Oxygen was taken as 4.0 and (OH) as 1.0 per formula unit. Note, however, that the oxygen weight percent was obtained by difference from 100% and its value depends critically on surface roughness, differences in the chemical surroundings of the

elements between the standards and the sample, and other specimen-related factors. For comparison, Table 4 shows several other chemical analyses of the anhydrous components, demonstrating substantial solid solution in austinite (Giuseppetti and Tadini, 1988; Jambor et al., 1980; Radcliffe and Simmons, 1971; Richmond, 1940). Pure Zn-, Cu-, and Mg-calcium end members have been synthesized (Richmond, 1940). Tables of observed and calculated structure factors are deposited in the editorial office.

Discussion

Arsenic tetrahedra, Zn octahedra, and Ca square antiprisms share edges and vertices to form a dense three dimensional framework (Fig. 1). Arsenic

L. A. CLARK *ET AL.*

TABLE 4. Comparison of chemical analyses of austinite (wt.%)

	This study	[1]	(A1) [2]	(A3) [2]	(A7) [2]	[3]	[4]
CaO	20.9	21.3	21.1	21.8	21.5	19.2	20.2
ZnO	28.4	30.1	30.7	30.6	29.9	32.5	28.5
CuO	0.91	0.88	–	–	1.2	–	–
MgO	0.3	–	0.3	0.6	0.2	–	1.3
MnO	–	–	–	–	–	–	3.9
FeO	–	0.49	–	–	–	–	0.47
As_2O_5	42.4	42.8	43.9	43.1	43.8	42.7	43.2
P_2O_5	–	0.9	–	–	–	0.10	–
Sum:	92.9	96.5	96	96.1	96.6	94.5	97.6

[1] Giuseppetti and Tadini, 1988
[2] Radcliffe and Simmons, 1971
[3] Richmond, 1940
[4] Dunn, 1979

coordinates with O (1—4) at the vertices of an almost regular tetrahedron. Two OH groups [O(5)] on opposing vertices, O(4), O(3) and two O(1) form a slightly distorted octahedron around Zn. The Ca atom coordinates with one OH, two O(2), two O(3), two O(4), and one O(1) to create a distorted square antiprism.

The As tetrahedra are not linked to each other, but share edges O(1)—O(2) and O(2)—O(4) with the Ca square antiprisms. The O(1), O(3), and O(4) vertices are shared with Zn octahedra. Because the average As-O bond distance 1.694 Å is shorter than the predicted distance for ionic bonding of 1.72 Å (Shannon, 1976), considerable covalency is indicated.

The geometry of the H-bond to O(2) indicates strength (reviews: Brown, 1976; Hawthorne, 1992): length 1.91(3) Å, H—O(5) angle 167(3)°, and O(2)—O(5) distance 2.723(2) Å.

The Zn octahedra are linked by their O(1)-OH edges, forming independent chains parallel to the *c* screw axis. These chains are linked by As tetrahedra, which share vertices, and Ca square antiprisms which share O(1)—O(4), O(4)—O(5), and O(3)—O(5) edges with the Zn octahedra. The average of the 2.095 to 2.240 Å Zn—O bond distances is 2.106 Å.

The Ca square antiprisms occupy most of the space between the Zn chains, sharing two edges with As tetrahedra, and three edges with Zn octahedra. They are linked to each other along their two O(3)—O(4) edges to form chains running parallel to the *a* screw axis. The O(2) vertices link these chains creating pseudohexagonal 'channels' occupied by the Zn octahedral chains (Fig. 2). The average of the 2.449 to 2.661 Å Ca—O bond distances is 2.525 Å.

The present Zn—Zn distance in austinite of 2.977 Å (= *c*/2 = 5.934/2), compares with the Cu—Cu distance in conichalcite of 2.92 Å (Qurashi and Barnes, 1963*a*). The lower *c* = 5.921(1) Å reported by Giuseppetti and Tadini (1988) for austinite might imply Cu substitution, if the reported errors in the cell dimensions are unbiased by systematic error.

A bond valence analysis, which incorporated the O H...O(2) H-bond, indicated that the O(5) atom is slightly underbonded. Because the OH group is coordinated with Zn, the formula CaZn(OH)(AsO$_4$) is appropriate for austinite (Sumin De Portilla, 1974).

The structure of austinite is described by Eby and Hawthorne (1993) as a M=M-T framework structure (edge-sharing octahedral chains linked by tetrahedral vertices). It is very similar to that of the minerals in the descloizite group which are essentially the vanadate counterparts of the adelite group (Qurashi and Barnes, 1963*b*; Basso *et al.*, 1989). Descloizite group minerals differ structurally from austinite (and the adelite group minerals in general) in that: (1) the interatomic distances for descloizite group minerals are generally slightly larger, caused by differences in the ionic radii for V^{+5} and As^{+5} (0.59 and 0.34 Å respectively); and (2) in some minerals, the structure has been refined with the space group *Pnma* instead of $P2_12_12_1$, due to small shifts in the coordinates of the atoms. The structural similarity between these two groups, and the solid substitution involving the cations within the groups, indicates that these minerals are probably end-members in a complex isomorphic series.

To conclude, the present structure determination confirms the earlier structure of austinite, and
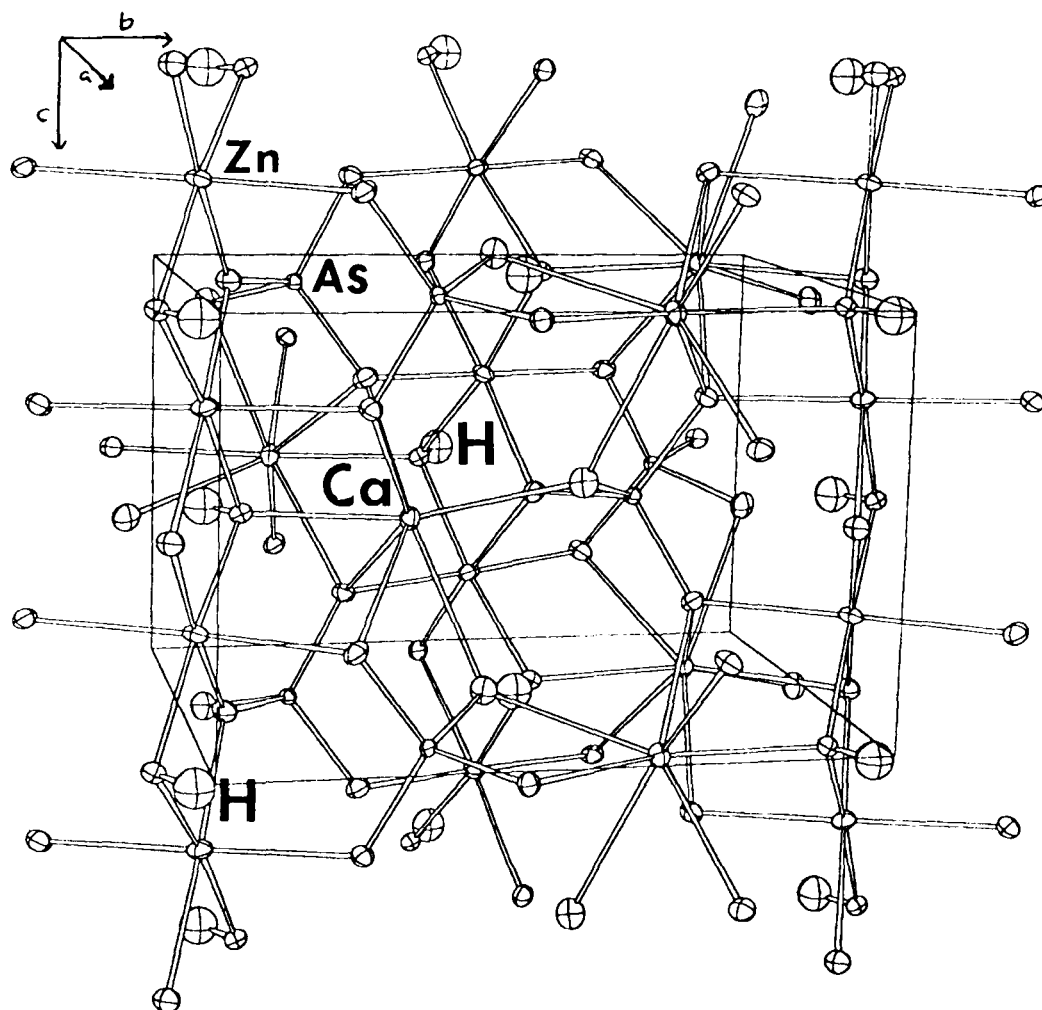
FIG. 1. Model of austinite looking down the a axis. Edge-shared Zn octahedral chains run parallel to the c axis (vertical).

provides higher accuracy and an absolute configuration. The details of the interatomic distances and angles are interpretable semiquantitatively in terms of current models of chemical bonding. We plan to use the Geo/Soil/Enviro-CARS experimental facility at the Advanced Photon Source to explore the crystal chemistry of austinite and other arsenate minerals using ~100 keV polarized X-ray photons. In addition, we should be able to quantify the stereochemical adsorption of arsenic species on mineral surfaces relevant to geochemical and environmental matters.

References

Basso R., Palenzona, A. and Zefiro, L. (1989) Crystal structure refinement of a Sr-bearing term related to copper vanadates and arsenates of adelite and descloizite groups. *Neues Jahrb. Mineral. Mh.*, 300–8.
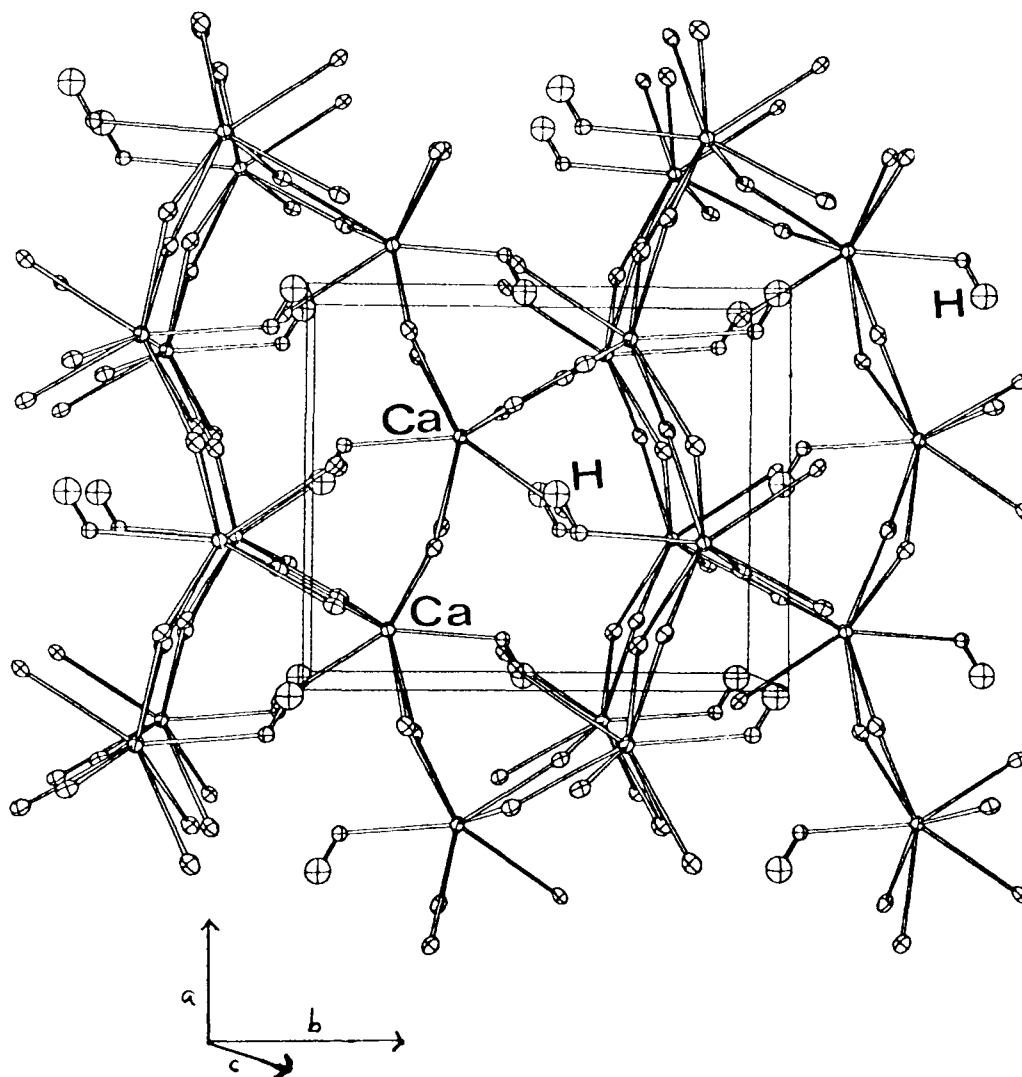
FIG. 2. Model of austinite down the *c* axis, showing only Ca atoms with the coordinating oxygen atoms. The Ca chains run parallel to the *a* axis, and pseudohexagonal channels are formed by shared vertices.

Brown, I.D. (1976) On the geometry of O — H...O hydrogen bonds. *Acta Crystallogr.,* **A32**, 24—31.

Cesbron, F.P., Ginderow, D., Giraud, R., Pelisson, P. and Pillard, F. (1987) La nickelaustinite Ca(Ni,Zn)(AsO₄)(OH): nouvelle espèce minérale du district cobalto-nickelifère de Bou-Azzer, Maroc. *Canad. Mineral.,* **25**, 401—7.

Crowley, J.A. (1975) The mineralogy of the Zinc Hill Mine, Inyo County, California. *Mineral. Record,* **6(3)**, 110—3.

Dunn, P.J. (1979) Contributions to the mineralogy of Franklin and Sterling Hill, New Jersey. *Mineral. Record,* **10(3)**, 160—5.

Eby, R.K. and Hawthorne, F.C. (1993) Structural relations in copper oxysalt minerals. I. Structural hierarchy. *Acta Crystallogr.,* **B49**, 28—56.

Fleischer, M. (1987) *Glossary of Mineral Species,* 5th Ed. Mineralogical Record Inc.: Tucson.

Giuseppetti, G. and Tadini, C. (1988) The structure of austinite, CaZn(AsO₄)(OH) from Kamareza,

Laurion (Greece). *Neues Jahrb. Mineral. Mh.*, 159—66.

Hawthorne, F.C. (1992) The role of OH and H_2O in oxide and oxysalt minerals. *Zeits. Kristallogr.*, **201**, 183—206.

Jambor, J.L., Owens, D.R. and Dutrizac, J.E. (1980) Solid solution in the adelite group of arsenates. *Canad. Mineral.*, **18**, 191—5.

Magalhães, M.C.F., Pedrosa de Jesus, J.D. and Williams, P.A. (1988) The chemistry of formation of some secondary arsenate minerals of Cu(II), Zn(II) and Pb(II). *Mineral. Mag.*, **52**, 679—90.

Nickel, E.H. and Birch, W.D. (1988) Cobaltaustinite — A new arsenate mineral from Dome Rock, South Australia. *Austral. Mineral.*, **3**, 53—7.

Qurashi, M.M. and Barnes, W.H. (1963a) The structures of the minerals of the descloizite and adelite groups: IV - Descloizite and conichalcite (Part 2). The structure of conichalcite. *Canad. Mineral.*, **7**, 561—77.

Qurashi, M.M. and Barnes, W.H. (1963b) The structures of the minerals of the descloizite and adelite groups: V — Descloizite and conichalcite (Part 3). The

structure of descloizite. *Amer. Mineral.*, **48**, 23—39.

Radcliffe, D. and Simmons, W.B. (1971) Austinite: chemical and physical properties in relation to conichalcite. *Amer. Mineral.*, **56**, 1359—65.

Richmond, W.E. (1940) Crystal chemistry of the phosphates, arsenates and vanadates of the type $A_2XO_4(Z)$. *Amer. Mineral.*, **25**, 441—79.

Shannon, R.D. (1976) Revised effective ionic radii and systematic studies of interatomic distances in halides and chalcogenides. *Acta Crystallogr.*, **A32**, 751—67.

Sheldrick, G.M. (1993) SHELXL93. *Program for the Refinement of Crystal Structures* Univ. Gottingen, Deutschland.

Staples, L.W. (1935) Austinite, a new arsenate mineral, from Gold Hill, Utah. *Amer. Mineral.*, **20**, 112—9.

Sumin de Portilla, V.I. (1974) Infrared spectroscopic investigation of the structure of some natural arsenates and the nature of H-bonds in their structures. *Canad. Mineral.*, **12**, 262—8.